International Journal of Thermal Sciences 48 (2009) 1870–1875

Contents lists available at ScienceDirect

International Journal of Thermal Sciences

journal homepage: www.elsevier.com/locate/ijts

Lattice Boltzmann simulation of natural convection in an open ended cavity

A.A. Mohamad [a,*], M. El-Ganaoui [b], R. Bennacer [c]

[a] Dept. of Mechanical Engineering, Schulich School of Engineering, The University of Calgary, Calgary, AB, T2N 1N4, Canada
[b] University of Limoges, FST, SPCTS, UMR 6638 CNRS, France
[c] LEEVAM, LEEE University Cergy-Pontoise Rue d'Eragny, Neuville sur Oise, 95031 Cedex, France

ARTICLE INFO

Article history:
Received 4 October 2008
Received in revised form
9 February 2009
Accepted 10 February 2009
Available online 14 March 2009

Keywords:
Lattice Boltzmann method
Natural convection
Open cavity

ABSTRACT

Natural convection in an open ended cavity is simulated using Lattice Boltzmann Method (LBM). The paper is intended to address the physics of flow and heat transfer in open end cavities and close end slots. The flow is induced into the cavity by buoyancy force due to a heated vertical wall. Also, the paper demonstrated that open boundary conditions used at the opening of the cavity is reliable, where the predicted results are similar to conventional CFD method (finite volume method, FVM) predictions. Prandtl number (Pr) is fixed to 0.71 (air) while Rayleigh number (Ra) and aspect ratio (A) of the cavity are changed in the range of 10^4–10^6 and of 0.5–10, respectively. It is found that the rate of heat transfer deceases asymptotically as the aspect ratio increases and may reach conduction limit for large aspect ratio. The flow evaluation in the cavity starts with recirculation inside the cavity, as the time proceeds the flow inside the cavity communicates with the ambient.

1. Introduction

There is no need to say that Lattice Boltzmann Methods (LBM) are in high pace development and have become a powerful method for simulation fluid flow and transport problems for single and multiphase flows [1,2]. In this work, the method is applied for natural convection in open cavities. Natural convection in open cavies and slots are encountered in many engineering applications, such as solar thermal receiver, heat convection from extended surfaces in heat exchangers, solar collectors with insulated strips [3], etc. Few numerical simulations in open cavities were reported for aspect ratio of unity without inclinations [4–6] and with inclinations [7,8]. On the other hand few research papers have been published on experimental studies of buoyant flow in open cavities [9–11]. Effect of conduction (conjugate effect) long the boundaries of the cavities and radiative heat transfer on the heat transfer were addressed by [12–14]. Stability of flow in open cavities exposed to stratified media is addressed by [15]. It is found that homogenous flow is steady for the range of investigated parameters ($Ra = 5 \times 10^6$–1×10^{10}, $Pr = 0.7$). However, for a high Ra, the stratified flow exhibits low and high frequency signals of the same types as in a closed cavity flow. The mechanisms of those frequencies were identified.

Most of the mentioned works investigated natural convection in cavities of aspect ratio of unity. The effect of systematic analysis of aspect ratio on the physics of flow and heat transfer is missing from the literature, which is worth being investigated. The velocity field and temperature profile are unknown at the opening boundary prior to solution. Such a boundary condition has never been tested for LBM applications before, which will be addressed in the present work. First the predictions of LBM are compared with predictions of finite volume method. The effect of aspect ratio on the flow and heat transfer systematically investigated. Also, the flow evaluation in the cavity is discussed.

2. Method of solution

Standard D2Q9 for flow and D2Q4 for temperature, LBM method is used in this work [1]; hence only brief discussion will be given in the following paragraphs, for completeness.

The BGK approximation lattice Boltzmann equation without external forces can be written as,

$$f_i(\mathbf{X} + \mathbf{c_i}\Delta t, t + \Delta t) - f_i(\mathbf{X}, t) = \Omega_i \quad (1)$$

where f_i are the particle distribution is defined for the finite set of the discrete particle velocity vectors $\mathbf{c_i}$. The collision operator, Ω_i, on the right hand side of Eq. (1) uses the so called Bhatangar-Gross-Krook (BGK) approximation [2]. For single time relaxation, the collision term Ω_i will be replaced by:

* Corresponding author.
E-mail address: mohamad@ucalgary.ca (A.A. Mohamad).

1290-0729/$ – see front matter © 2009 Elsevier Masson SAS. All rights reserved.
doi:10.1016/j.ijthermalsci.2009.02.004

$$\Omega_i = -\frac{f_i - f_i^{eq}}{\tau} \tag{2}$$

where τ ($\tau = 1/\omega_m$) is the relaxation time and f_i^{eq} is the local equilibrium distribution function that has an appropriately prescribed functional dependence on the local hydrodynamic properties.

The equilibrium distribution can be formulated as [2]:

$$f_i^{eq} = \omega_i \rho \left[1 + 3\frac{\mathbf{c_i}\cdot\mathbf{u}}{c^2} + \frac{9}{2}\frac{(\mathbf{c_i}\cdot\mathbf{u})^2}{c^4} - \frac{3}{2}\frac{\mathbf{u}\cdot\mathbf{u}}{c^2}\right] \tag{3}$$

where $\mathbf{u}$ and ρ are the macroscopic velocity and density, respectively, and ω_i are the constant factors, for D2Q9 is given as,

$$\omega_i = \begin{cases} 4/9 & i = 0, \ \textit{rest particle} \\ 1/9 & i = 1,3,5,7 \\ 1/36 & i = 2,4,6,8 \end{cases}. \tag{4}$$

The discrete velocities, $\mathbf{c_i}$, for the D2Q9 (Fig. 1) are defined as follows:

$$\begin{aligned} &\mathbf{c}_0 = (0,0) \quad \mathbf{c}_k = c(\cos\theta_k, \sin\theta_k) \quad \theta_k = (k-1)\pi/2 \\ &\textit{for} \quad k = 1,2,3,4 \mathbf{c}_k = c\sqrt{2}(\cos\theta_k, \sin\theta_k) \quad \theta_k \\ &\qquad = (k-5)\pi/2 + \pi/4 \quad \textit{for} \quad k = 5,6,7,8 \end{aligned} \tag{5}$$

where $c = \Delta x/\Delta t$, Δx and Δt are the lattice space and the lattice time step size, respectively, which are set to unity. The basic hydrodynamic quantities, such as density ρ and velocity $\mathbf{u}$, are obtained through moment summations in the velocity space:

$$\rho(\mathbf{X}, t) = \sum_i f_i(\mathbf{X}, t) \tag{6}$$

$$\rho\mathbf{u}(\mathbf{X}, t) = \sum_i \mathbf{c_i} f_i(\mathbf{X}, t) \tag{7}$$

The macroscopic viscosity is determined by

$$\nu = \left[\tau - \frac{1}{2}\right] c_s^2 \Delta t \tag{8}$$

Where c_s is speed of sound and equal to $c/\sqrt{3}$

For scalar function (temperature), another distribution is defined,

$$g_k(x + \Delta x, t + \Delta t) = g_k(x,t)[1 - \omega_s] + \omega_s g_k^{eq}(x,t) \tag{9}$$

D2Q4 is used to model transport of heat, for details see reference [1].

The equilibrium distribution function can be written as,

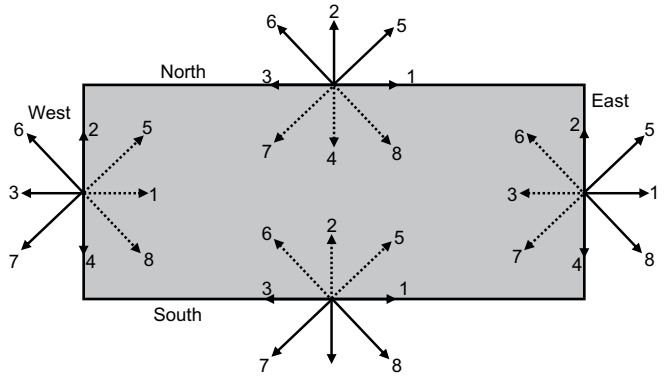

Fig. 1. Domain boundaries and direction of streaming velocities.

$$g_k^{eq} = w_k \phi(x,t)\left[1 + \frac{c_k \cdot u}{c_s^2}\right] \tag{10}$$

Notice that ω is different for momentum and scalar equations.

For momentum,

$$\omega_m = \frac{1}{3\cdot\nu + 0.5}, \tag{11}$$

where ν is the kinematic viscosity

and for the scalar

$$\omega_s = \frac{1}{2\cdot\alpha + 0.5}, \tag{12}$$

where α is the diffusion coefficient (thermal diffusion coefficient).

Nusselt number is calculated as,

$$Nu = -\frac{\partial T}{\partial Y} \tag{13}$$

Nusselt number is based on the height of the cavity, H. T stands for dimensionless temperature. Average Nusselt number is calculated by integrating eq. (13) along the height of the cavity and dividing by number of lattices along the height.

The standard LBM consists of two steps, streaming and collision. D2Q9 is used to solve the velocity field and D2Q4 is used to solve for the temperature field. The number of lattices used in x- and y-direction depends on the aspect ratio. However, at least 100 lattices are used in y-direction and number of lattice in x-direction is aspect ratio multiplied by the number of lattices in the y-direction. The buoyancy force term is added as an extra source term to equation (1), as,

$$F_b = 3 w_k g \beta \Delta T \tag{14}$$

where g, β and ΔT are gravitational acceleration, thermal expansion coefficient and temperature difference.

3. Boundary conditions

The distribution functions out of the domain are known from the streaming process. The unknown distribution functions are those toward the domain. Fig. 1 shows the unknown distribution function, which needs to be determined, as dotted lines.

Flow:

Bounce back boundary condition is used on the solid boundaries (west, north and south boundaries). At the east open boundary, the following condition is used,

$$f_{6,n} = f_{6,n-1}, \quad f_{3,n} = f_{3,n-1} \ \textit{and} \ f_{7,n} = f_{7,n-1} \tag{15}$$

Where n is the lattice on the boundary and $n-1$, is the lattice inside the cavity adjacent to the boundary.

Temperature:

Bounce back boundary condition (adiabatic) is used on the north and south of the boundaries. Temperature at the west wall is know, $T_w = 1.0$. Since we are using D2Q4, the only unknown is g_1, which is evaluated as,

$$g_1 = 0.5\, T_w - g_3 \tag{16}$$

The boundary condition for east wall needs special treatment, since prior to solution, the advected velocity direction is not known. It is assumed that if the flow is penetrating into the cavity, then the temperature should be ambient, $T = 0$, and if the flow leaving the

Table 1
Average Nusselt number comparison predicted by different methods.

Ra	LBM (present), Pr = 0.71	Mohamad [7] (FV), Pr = 0.71	Hinojosa et al. [13] (FV), Pr = 1.0
10^4	3.377	3.264	3.57
10^5	7.323	7.261	7.75
10^6	14.380	14.076	15.11

cavity, it is assumed that there is no heat diffusion, i.e., gradient of temperature is negligible.

For east boundary, the distribution function, g_3 is evaluated as,

$$if\ u < 0\ then\ g_{3,n} = 0 - g_{1,n} \tag{17a}$$

$$if\ u > 0\ then\ g_{3,n} = g_{3,n-1} \tag{17b}$$

4. Results and discussion

Table 1 summarizes the average Nusselt numbers predicted by LBM and compared with predictions of Finite Volume method (FVM) for aspect ratio of one with results of [7,13]. Also, the streamlines and isotherms for both methods gave same results. Hence, it is concluded that LBM with the suggested boundary condition at the opening of the cavity can produce reliable results. Fig. 2 shows streamlines for $Ra = 10^4$ for different aspect ratios. The flow enters from the lower half portion of the cavity and leaves from the upper half of the opening for all aspect ratios. It is clear that the flow becomes one dimensional for $As = 4$ and for $x/H > 1.0$. Hence, an analytical solution is possible for high aspect ratios ($As > 4.0$). In another words, Navier–Stokes equation can be

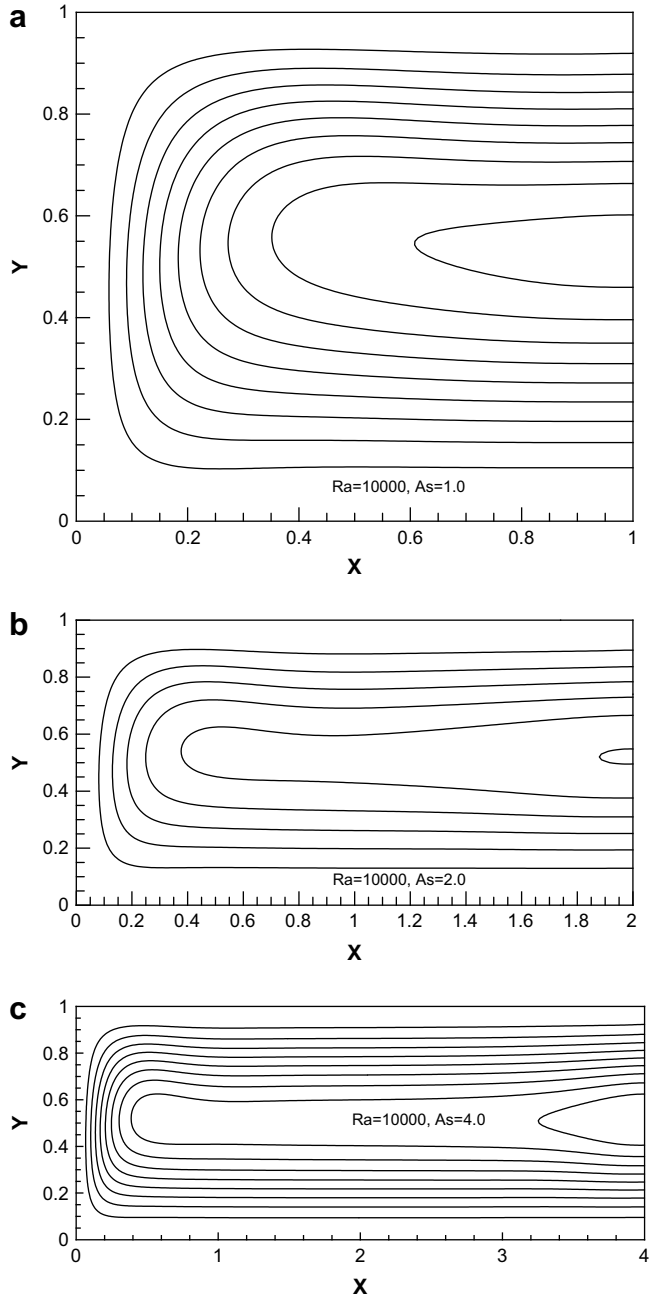

Fig. 2. a, Streamlines for $Ra = 10^4$ and aspect ratio of 1.0. b, Streamlines for $Ra = 10^4$ and aspect ratio of 2.0. c, Streamlines for $Ra = 10^4$ and aspect ratio 4.0.

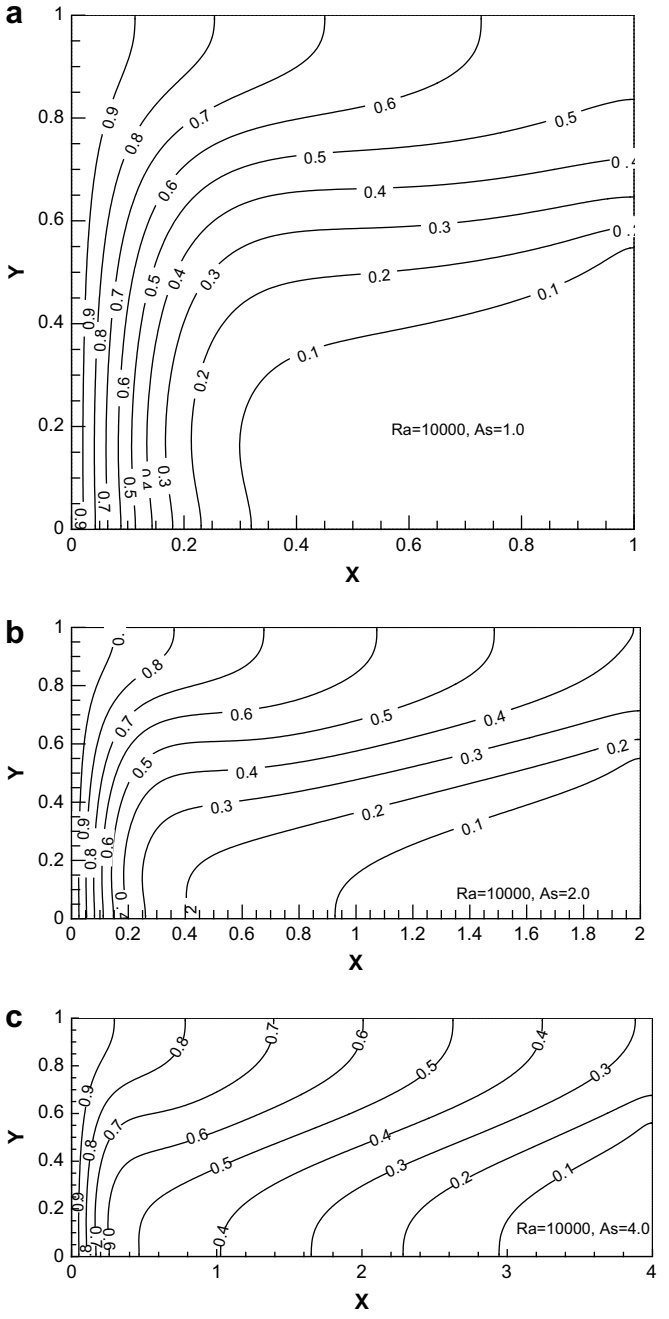

Fig. 3. a, Isotherms for $Ra = 10^4$ and aspect ratio of 1.0. b, Isotherms for $Ra = 10^4$ and aspect ratio of 2.0. c, Isotherms for $Ra = 10^4$, aspect ratio of 4.0.

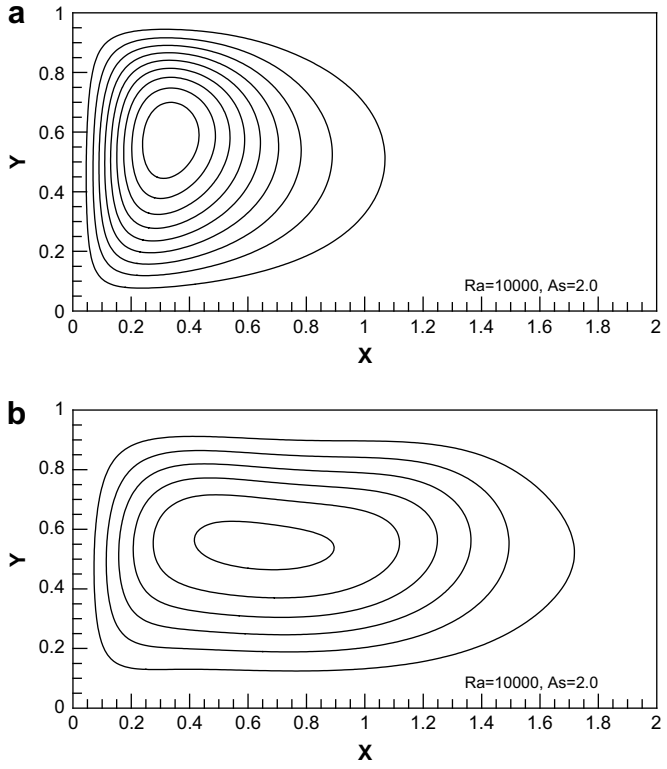

Fig. 4. a, Streamlines for $Ra = 10^4$ and aspect ratio of 2.0 at early stage of developments. b, Streamlines for $Ra = 10^4$ and aspect ratio of 2.0 at intermediate stage of developments.

simplified and solved analytically with constrain that the net flow is zero. Isotherms for aspect ratio of are shown in Fig. 3. For aspect ratio of 4, the isotherms at the upper half of the cavity show that the temperature gradient is almost constant along the cavity, where the isotherms are equally spaced. However, this is not the case for low aspect ratio. Hence, it is expected that by increasing aspect ratio, the rate of heat transfer decreases asymptotically to conduction limit. Fig. 4 shows the average rate of heat transfer as a function of

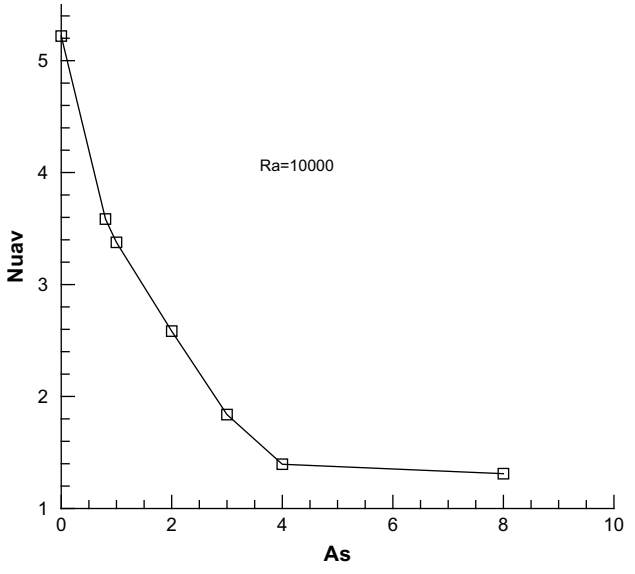

Fig. 5. Average Nusselt as a function of aspect ratio for $Ra = 10^4$.

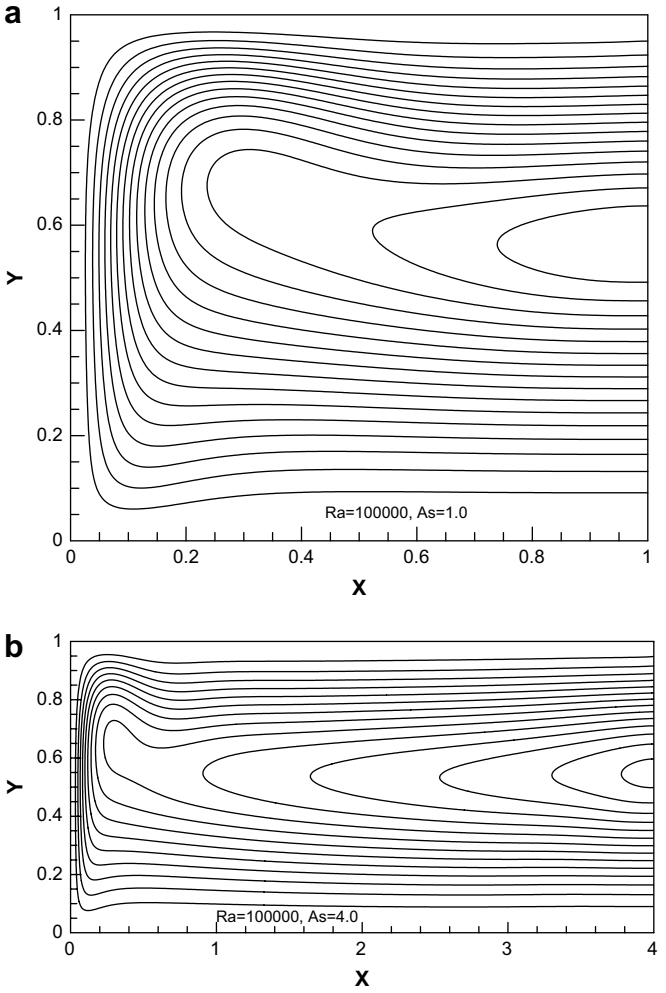

Fig. 6. a, Streamlines for $Ra = 10^5$ and aspect ratio of 1.0. b, Streamlines for $Ra = 10^5$ and aspect ratio of 4.0.

aspect ratio. The rate of heat transfer is maximum for a flat plate and decreases as the aspect ratio increases due to hydraulic resistance, shear stress, added by the horizontal boundaries. The rate of heat transfer, Nusselt number is expected to reach asymptotically conduction limit as the aspect ratio increases, as mentioned before. The scenario of flow development inside of the cavity is that at the early stage, the buoyancy force creates recirculation inside the cavity. At this stage there is no communication between the flows inside of the cavity and ambient, i.e., no flow enters the cavity from the outside. As the time proceeds, the recirculation elongates and finally communication begins between the flow in the cavity and the ambient. The time needed for flow inside the cavity to communicate with the ambient depends on the aspect ratio and Ra number, as the aspect ratio increase and/or Ra decreases the time needed for communication increases. Fig. 5 shows snap shots at early and intermediate stages of flow development inside the cavity for $Ra = 10^4$ and aspect ratio of 2.0.

Results for $Ra = 10^5$ are displayed in Fig. 6, which shows streamlines for selected aspect ratios. The unique feature of the streamline compared with the results of $Ra = 10^4$, is that the streamlines are tilted upward at the upper corner of the closed end of the cavity due to strong buoyancy force, which forms a wall jet. However, the strength of the buoyancy is not enough to form recirculation zone at the corner. Fig. 7 shows corresponding

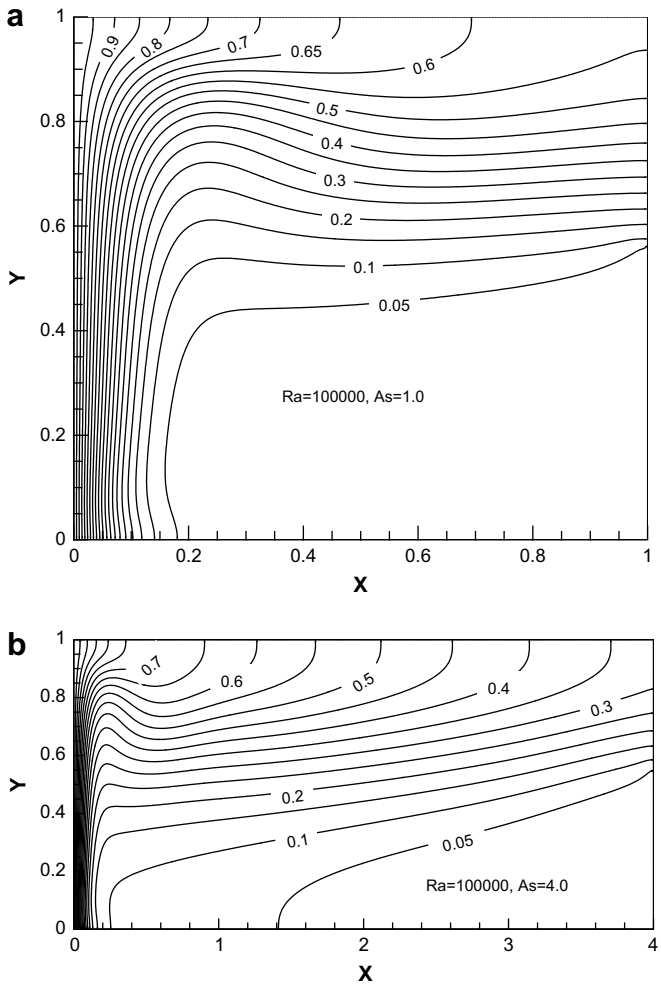

Fig. 7. a, Streamlines for $Ra = 10^5$ and aspect ratio of 1.0. b, Isotherms for $Ra = 10^5$ and aspect ratio of 4.0.

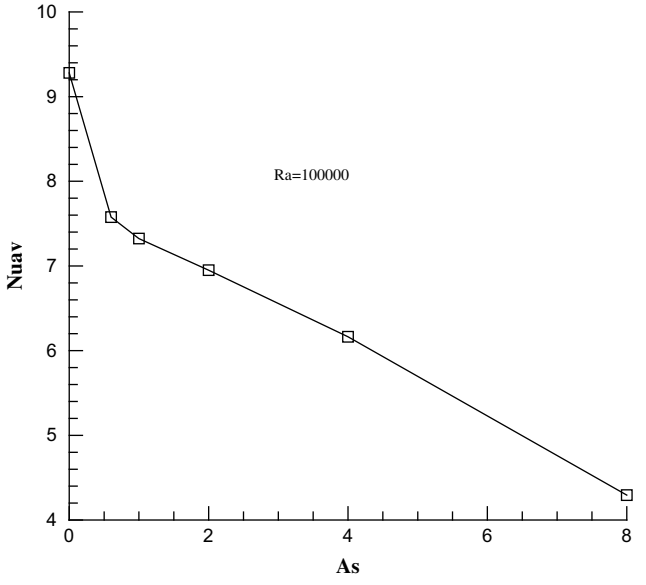

Fig. 8. Nusselt number as a function of aspect ratio for $Ra = 10^5$.

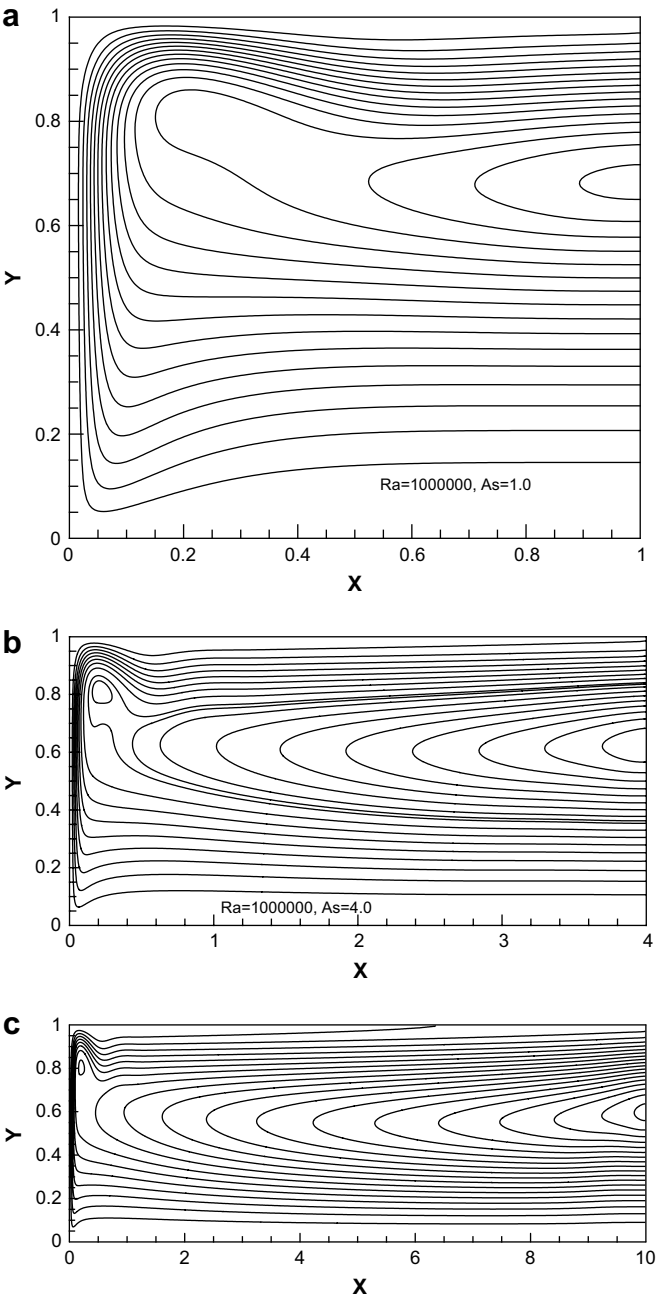

Fig. 9. a, Streamlines for $Ra = 10^6$ and aspect ratio of 1.0. b, Streamlines for $Ra = 10^6$ and aspect ratio of 4.0. c, Streamlines for $Ra = 10^6$ and aspect ratio of 10.0.

isotherms for $Ra = 10^5$. For aspect ratio of 4.0, the isotherm lines are not evenly distributed as for $Ra = 10^4$. As the Ra increases the aspect ratio for a developed flow conditions increases. Average Nusselt number as a function of aspect ratio is shown in Fig. 8. The rate of heat transfer exponentially decreases as the aspect ratio increases for the investigated range of aspect ratio.

Further increase of Ra to 10^6, increase buoyancy force and flow may form recirculation at the upper corner of the closed end of the cavity, Fig. 9. Isotherms shows that the flow is mainly stratified at the upper half of the cavity and the flow almost isothermal at the lower half of the cavity, Fig. 10. Fig. 11 shows average Nusselt number as function of aspect ratio. Nusselt number somehow linearly decreases as the aspect ratio increase from 2.0 to 10.0. However, this may be due to the scaling of aspect ratio axis.

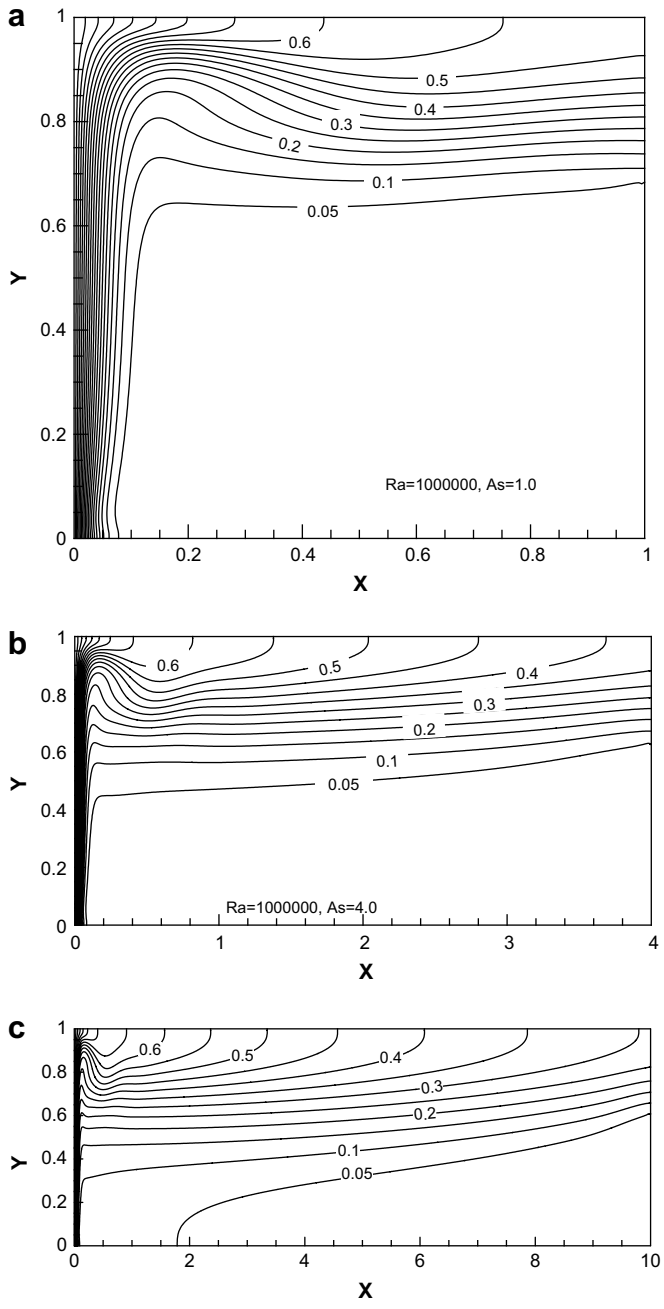

Fig. 10. a, Isotherms for $Ra = 10^6$ and aspect ratio of 1.0. b, Isotherms for $Ra = 10^6$ and aspect ratio of 4.0. c, Isotherms for $Ra = 10^6$ and aspect ratio of 10.0.

5. Conclusions

Buoyancy driven flows in open cavities were studied using LBM for a range of controlling parameters. The suggested boundary condition for LBM seems to be appropriate for open boundary condition without prior knowledge of the flow direction. The flow evolution in the cavity is explained, at the early stage of flow development inside the cavity forms a recirculation and as time proceeds, the re-circulated flow communicates with the ambient. As the aspect ratio increase and/or Ra decrease the time needed for flow inside the cavity to communicate with the ambient increase.

Increasing aspect ratio for a given Ra decreases the rate of heat transfer up to the conduction limit.

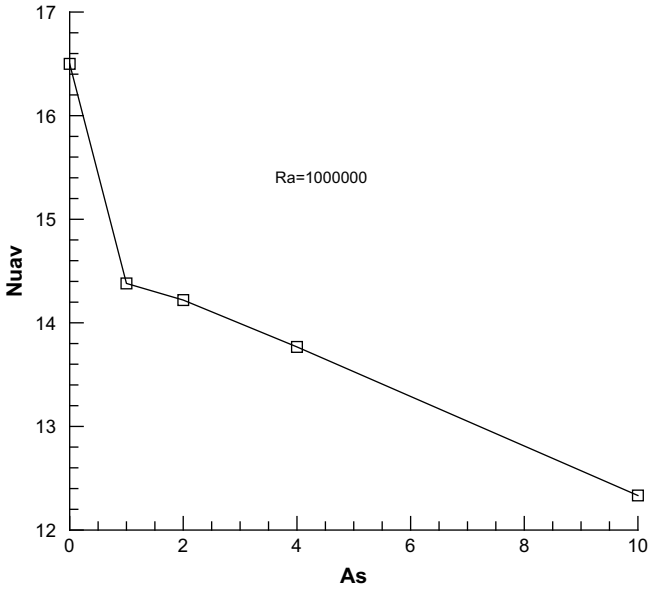

Fig. 11. Nusselt number as a function of aspect ratio for $Ra = 10^6$.

References

[1] A.A. Mohamad, Applied Lattice Boltzmann Method for Transport Phenomena, Momentum, Heat and Mass Transfer, Sure, Calgary, 2007.
[2] S. Succi, The Lattice Boltzmann Equation for Fluid Dynamics and Beyond, Clarendon Press, Oxford, London, 2001.
[3] I. Sazia, A.A. Mohamad, Suppressing free convection from a flat plate with poor conductor ribs, Int. J. Heat Mass Transfer 42 (1) (1999) 2041–2051.
[4] P. Le Quere, J.A.C. Humphrey, F.S. Sherman, Numerical calculation of thermally driven two-dimensional unsteady laminar flow in cavities of rectangular cross section, Numer. Heat Transfer 4 (1981) 249–283.
[5] F. Penot, Numerical calculation of two-dimensional natural convection in isothermal cavities, Numer. Heat Transfer 5 (1982) 421–437.
[6] Y.L. Chan, C.L. Tien, A numerical study of two-dimensional natural convection in square open cavities, Numer. Heat Transfer 8 (1985) 65–80.
[7] A.A. Mohamad, Natural convection in open cavities and slots, Numer. Heat Transfer 27 (1995) 705–716.
[8] O. Polat, E. Bilgen, Laminar natural convection in inclined open shallow cavities, Int. J. Therm. Sci. 41 (2002) 360–368.
[9] Y.L. Chan, C.L. Tien, Laminar natural convection in shallow open cavities, J. Heat Transfer 108 (1986) 305–309.
[10] E. Bilgen, Passive solar massive wall systems with fins attached on the heated wall and without glazing, J. Sol. Energ. Eng. 122 (2000) 30–34.
[11] S.S. Cha, K.J. Choi, An interferometric investigation of open cavity natural convection heat transfer, Exp. Heat Transfer 2 (1989) 27–40.
[12] O. Polat, E. Bilgen, Conjugate heat transfer in inclined open shallow cavities, Int. J. Heat Mass Transfer 46 (2003) 1563–1573.
[13] J.F. Hinojosa, R.E. Cabanillas, G. Alvarez, C.E. Estrada, Nusslet number for the natural convection and surface thermal radiation in a square tilted open cavity, Int. Comm. Heat Mass Transfer 32 (2005) 1184–1192.
[14] N. Nouanegue, A. Muftuoglu, E. Bilgen, Conjugate heat transfer by natural convection, conduction and radiation in open cavities, Int. J. Heat Mass Transfer (2008).
[15] A. Javam, S.W. Armfield, Stability and transition of stratified natural convection flow in open cavities, J. Fluid Mech. 44 (2001) 285–303.